

## What Can We Learn About the Ionosphere Using the EISCAT Heating Facility?

**Michael T. Rietveld**  
EISCAT Scientific Association  
Ramfjordmoen  
N-9027 Ramfjordbotn  
[mike.rietveld@eiscat.uit.no](mailto:mike.rietveld@eiscat.uit.no)

### **ABSTRACT**

*Apart from being used for plasma physics, the HF facility near Tromsø, Norway, can be used to perturb the ionosphere at various heights in different ways, thereby giving information about the ionosphere, atmosphere and even magnetosphere. The co-located incoherent scatter radars are probably the most powerful instrument for probing the ionosphere, but HF techniques can complement the radars and even have some advantages. The principal perturbation method is to increase the electron temperature in a controlled way, some examples of which are presented here.*

*Artificial electron heating in the E and F regions is useful for testing aeronomical models. More recently it has been discovered that electron heating can dramatically affect polar mesospheric echoes observed by VHF and UHF radars. Particularly the overshoot effect promises to be a powerful diagnostic of the physics and chemistry related to the formation of these layers, which are thought to involve dust, ice particles and aerosols.*

*Radio induced optical emissions provide a way of measuring the lifetimes of excited species at different heights in the ionosphere, thereby providing a way of measuring the neutral density which is one of the most important parameters determining the lifetime.*

*The technique of creating artificial periodic irregularities set up in the standing wave pattern of the up-going and ionospherically reflected HF wave provides valuable information all heights below reflection. One particular feature of this method is that it can detect the presence of layers around 50 km and measure vertical winds, and electron densities and temperatures at various heights.*

### **1.0 INTRODUCTION**

The use of Heating to diagnose the ionosphere started with the discovery of the Luxembourg effect by Tellegen in 1933 [1], and its explanation by Bailey and Martyn [2], namely that powerful LF or HF radio waves heat the electrons in the lower ionosphere and thereby affect the absorption coefficient of other radio waves. This led to the cross-modulation technique of probing the lower ionosphere, which was developed by Fejer [3], and which led to results by several groups which he reviewed in 1970 [4].

Dedicated powerful HF radio wave transmitting facilities have been in use since the 1970s to do both plasma physics and geophysical research. At present there are five operating facilities: HIPAS [5] and HAARP [6] in Alaska, EISCAT Heating in northern Norway [7], SPEAR on the island of Spitsbergen [8] and SURA in Russia [9]. Another important facility in Puerto Rico [10] was damaged by a hurricane in 1998 but there are plans to build a replacement. Although incoherent radar, which is sometimes co-located with these powerful HF facilities, is recognised as being the most powerful technique for measuring ionospheric and to some extent atmospheric properties, its capabilities can often be extended by using

ionospheric perturbation techniques. HF-modification facilities, which themselves are much less expensive than incoherent scatter radars, can also be used together with even less expensive HF or VHF coherent scatter radars or other diagnostics to probe the ionosphere and even magnetosphere as will be shown below.

By perturbing the ionosphere in a controlled way and measuring the effect with some other instrument, it is possible to learn something about the properties of the ionospheric plasma or the neutral atmosphere. There are several ways of causing a perturbation with a powerful HF radio wave. The absorption of the wave causes electron heating, which is perhaps the most direct way, and will be discussed in section 2. Another way is to directly excite plasma waves which are localised in their source height by resonance conditions. If the plasma waves are Langmuir or ion acoustic waves they can be measured by incoherent scatter radars and allow accurate calibration of electron densities and temperatures. The associated plasma turbulence can also energize electrons such that they cause the atmospheric molecules or atoms to emit light. These plasma wave effects are discussed in Sections 2 and 3. Modulated electron heating can be used to create low frequency ionospheric currents which are in turn useful for studying the properties of the ionosphere or the coupled ionosphere-magnetosphere system, as discussed in Section 4. Heating effects can also be used to track the ionospheric electric field of naturally-occurring ULF waves, as demonstrated in the same section. Finally, in Section 5 a technique is described where periodic irregularities set up in the standing wave of the reflected HF pump are used as a tracer for ionospheric parameters from the F region down to extremely low heights like 50 km.

## **2.0 ELECTRON HEATING**

A powerful HF is absorbed in the D region through collisions or simple Ohmic heating. Models predict temperature enhancements up to many hundreds or even thousands of degrees, but direct measurements of this by means of incoherent scatter radar has proved impossible to verify so far. Nevertheless the effects of electron heating at heights between about 60 and 90 km are evident in a variety of ways. Examples are the modulation of the electron collision frequency and hence conductivities and electric currents by amplitude modulated heating at frequencies from sub-Hz to kHz, as described in Section 4. Heating effects in the E region also exist but have also been difficult to measure [11]. Heating effects in the F region can be strong through anomalous absorption of the HF wave caused by electrostatic instabilities, and have been well documented [12], [13]. We now discuss the diagnostic applications of D, E and F region heating.

### **2.1 The cross-modulation effect**

As mentioned earlier, the cross-modulation technique was developed out of the accidental discovery of the Luxembourg effect to become one of very few techniques for measuring the electron collision frequency and density of the lower ionosphere from about 70 to 90 km [3][4]. In the technique the amplitude and sometimes phase of a pulsed ‘wanted’ wave is measured after reflection from the ionospheric E or F-region. A ‘disturbing’ or heating wave of say 150  $\mu$ s, on another frequency is transmitted at half the rate of the wanted signal at a variable time delay after the wanted pulse such that the up-going heating wave meets the down-coming wanted wave at a desired height,  $h$ , as illustrated in Figure 1, panels a and b. The change in amplitude (and sometimes phase), or cross-modulation coefficient is measured as a function of height and from the theory the electron density and electron collision frequency are obtained.

A variation of this experiment, called ‘complementary cross modulation’, has been suggested by M. Sulzer [14] to measure the heating effects of powerful HF radio waves on the D-region densities on the long timescales (seconds and minutes) necessary to affect the chemical reaction rates. This is something that is difficult to do with other techniques. After a very preliminary experiment [14] however, this seems not to have been followed up. Figure 1, (panel c), shows this variant where one replaces a disturbing pulse by a gap of the same length in a very long heating pulse. I suggest that it is time to revisit this technique using

the modern HF facilities and signal processing techniques available today.

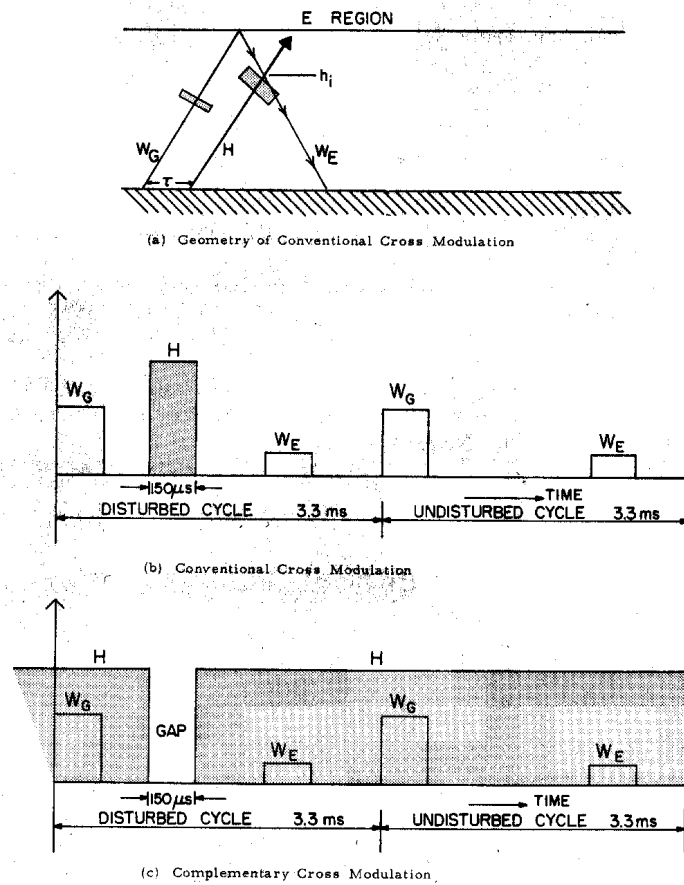


Figure 1: Geometry and pulse sequence for conventional (panels a and b) and complementary modes (panel c) of cross modulation. Taken from [14].

## 2.2 The effect of electron heating on the mesosphere

The mesosphere is that region of the atmosphere between about 50 and 85 km where the temperature decreases with altitude and reaches a minimum at around 85 km. It is difficult to access this region except through sounding rockets or radars. Radar echoes require sufficient electron density which is provided through ionising sunlight, precipitating energetic electrons from magnetospheric acceleration processes such as that associated with the aurora, or protons during energetic solar eruptions. When there are sufficient electrons, they can be structured on various spatial scales by turbulence, or by attachment to aerosols such as ice and dust particles, thereby acting as passive tracers of the neutral atmosphere and its inhomogeneities. Strong VHF and occasionally UHF radar echoes which are seen commonly in the polar mesosphere at heights from 80 to 90 km, known as Polar Mesospheric Summer Echoes (PMSE) [15][16] are still not understood. Weaker and rarer echoes are also seen from lower heights around 70 km, sometimes termed Polar Mesosphere Winter Echoes (PMWE) [17].

Chilson et al. [18] found that the strength of PMSE echoes could be weakened by up to 10 dB by transmitting a powerful HF wave having an effective radiated power (ERP) of several hundred MW. The response time was practically instantaneous [19] suggesting that electron heating, which has a time

constant of tens to hundreds of microseconds in these heights [20], caused the weakening of the echoes. This weakening is caused by the increased diffusivity of the hotter electrons smearing out the small meter-scale structuring of the electrons [21]. More recently O. Havnes predicted that that by using a lower duty cycle modulation, it should also be possible to enhance the strength of the echoes [22]. The effect which was immediately found [23] and which is shown in Figure 2, promises to be an important diagnostic of the mesosphere and D region. This is because, as Figure 3 shows, the overshoot characteristic curve depends on the aerosol size used in the model. Figure 3 shows two cases computed for a plasma density  $n_0 = 4 \times 10^9 \text{ m}^{-3}$  and an increase in the electron temperature from a background value of 150 K, to 390 K with heating. The level of suppression (0 to 1 in Figure 3) depends on the temperature enhancement. Two different dust sizes were used in the figure. The dust density is  $n_d = 10^9 \text{ m}^{-3}$  for the case with particles of radius  $r = 10 \text{ nm}$  (solid line) and  $n_d = 4 \times 10^7 \text{ m}^{-3}$  for the 50 nm large particles (dashed line).

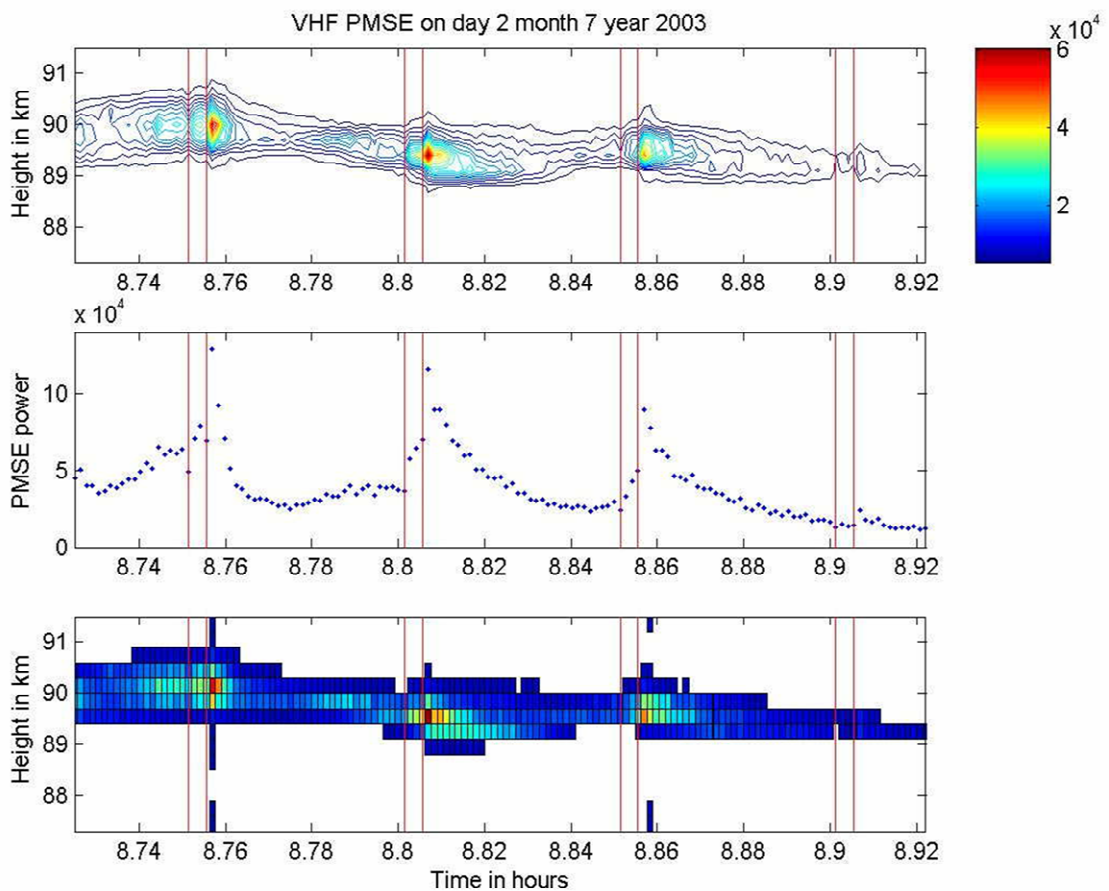


**Figure 2: PMSE echo strength showing an overshoot immediately after switching the 3s long heater pulse off. HF-on is shown by the vertical lines. The bottom panel shows the raw data, corrected for radar transmitter power, while the upper panel shows the same data but now smoothed. The relative intensity scale is the same for both panels, and the background noise on this linear scale is at approximately 2500. The middle panel shows the sum of the three highest intensities at each time sample and is a measure of the total PMSE intensity as a function of time. Taken from [23].**

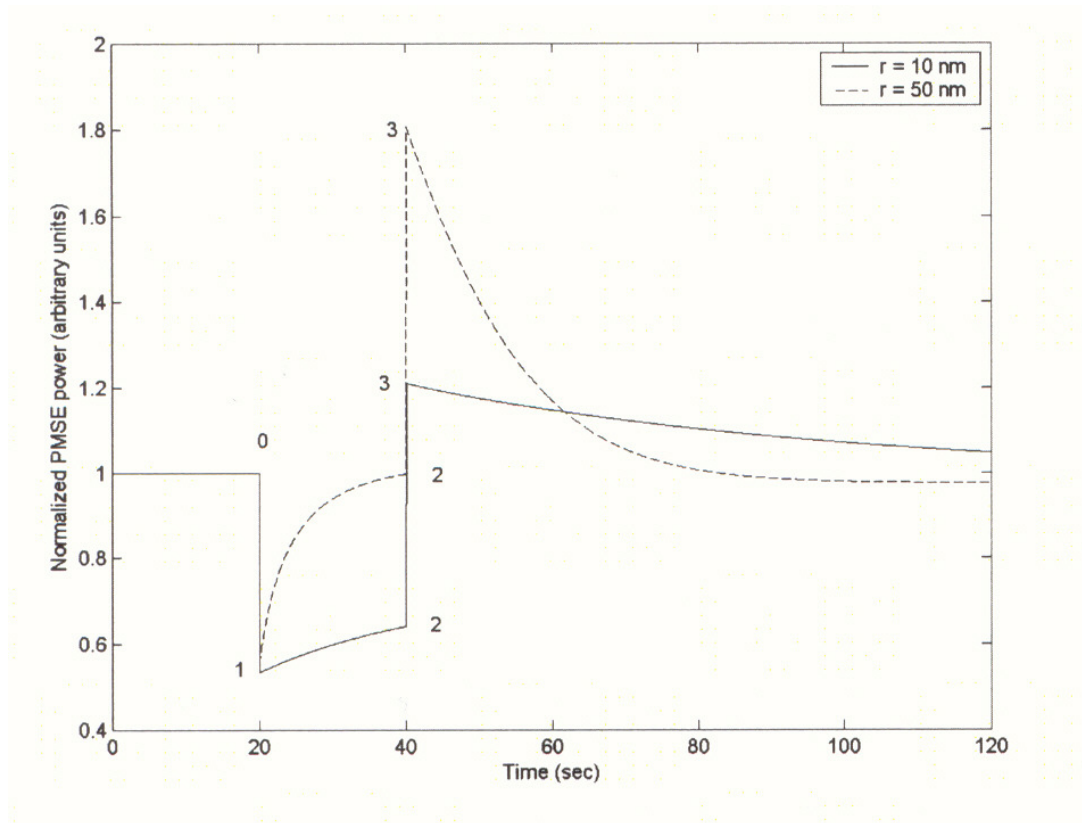


Figure 3: Model calculations showing how the shape of the overshoot phenomenon depends on particle size. HF is on from 20 to 40 s and the amplitude from 0 to 1 depends on the electron heating. Taken from [23].

### 2.3 Heating and possibly cooling effects in the E region

There have been very few reported measurements of HF-induced electron heating effects in the E region. This is probably because the heating effects are weaker and intrinsically more difficult to measure because of the shorter scale height. There have been some interesting results published [11] however, which are surprising at first sight. Heating of electrons was found under weak electrojet conditions at heights between 100 and 135 km, as might be expected from absorption of the HF waves. However, under strong electrojet conditions and slightly underdense heating (the HF frequency being greater than the maximum plasma frequency), HF heating appeared to reduce the electron temperature between 100 and 115 km, whilst still increasing the temperature above the electrojet in the 120-135 km range. The proposed explanation is that under strong electrojet conditions the Farley-Buneman instability is the main source of electron heating, but the HF waves can cause a reduction in the amplitude of the Farley-Buneman waves [11] and hence in the overall heating. Although there are few measurements, they should encourage further attempts at studying E-region heating and the Farley-Buneman instability by using HF-induced perturbations.

### 2.4 Heating effects in the F region

Measurements of HF-induced electron heating in the F region were first analysed in detail by Mantas et al. [12]. Such measurements provide useful tests of models of the thermal balance of the electron and ion gas

# What Can We Learn About the Ionosphere using the EISCAT Heating Facility?

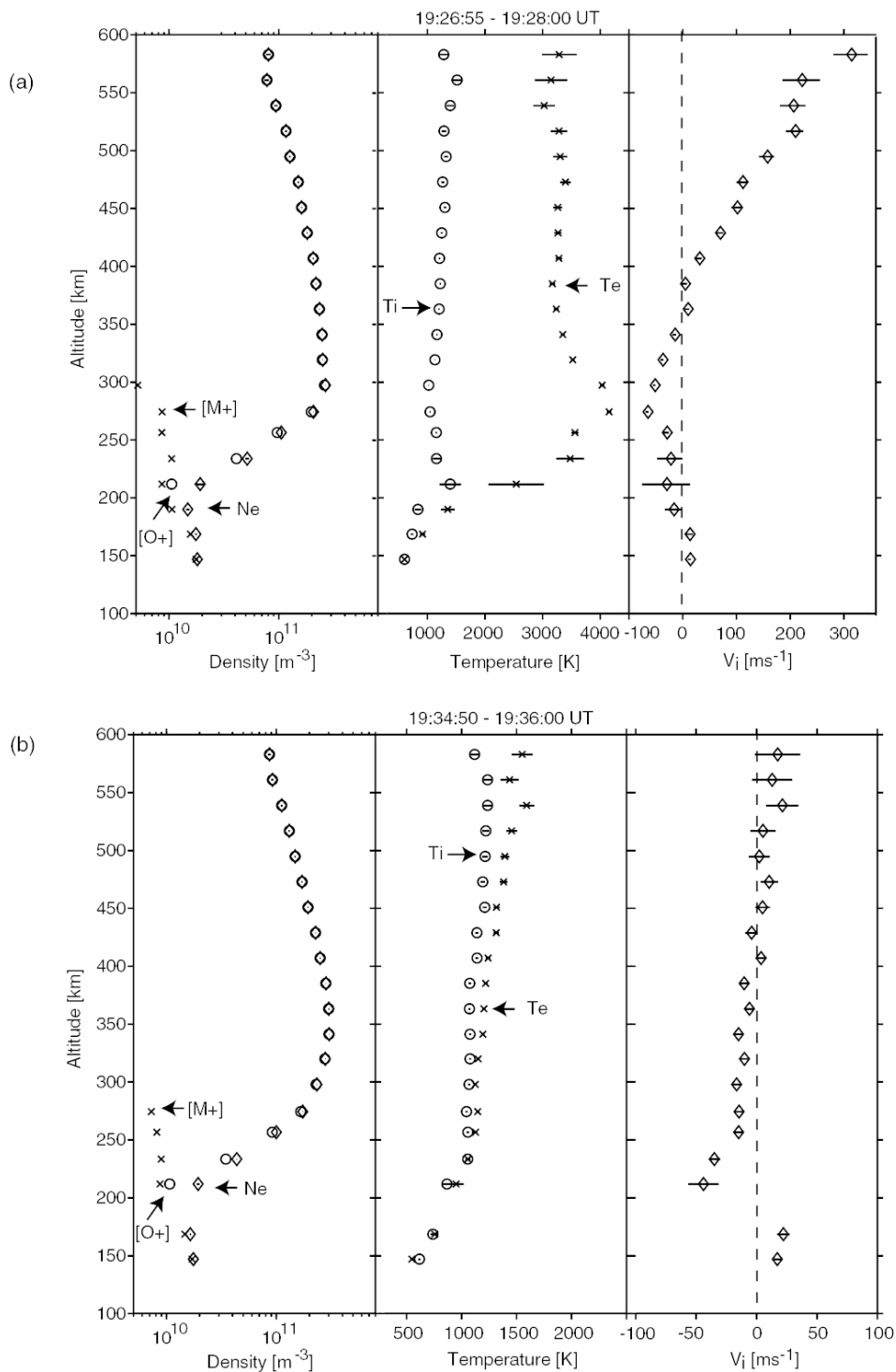


**Figure 4: EISCAT UHF data for two selected time intervals from 7 October 1999, showing electron density (Ne), ion and electron temperatures (Ti, Te), and ion velocity ( $V_i$ ) for two field-aligned positions. (a) An interval starting about 3 minutes after HF pump on directed along the magnetic field, showing the largest elevated electron temperatures and ion outflows. (b) An interval starting about 3 minutes after HF pump off, showing the background values. The  $O^+$  and  $M^+$  (molecular ion) densities are from a model. From [13]**

in the ionosphere. If one neglects particle concentration changes then only the coupled time-dependent heat equations for the electron and ion gas need to be solved. A large error in the assumed electron energy loss rates through the various collision mechanisms can be detected by comparing the observed with the calculated decay rate of the enhanced electron temperature profile after turning the HF wave off [12]. Earlier daytime heating results of temperature enhancements of up to 55% were presented and modelled by Stocker et al. [24], but more recently experiments at night have shown much larger temperature enhancements [28][13].

The electron heating also leads to some weak ion and some neutral gas heating, and to ion outflows [13] as shown in Figure 4. Such ion outflows have been predicted theoretically and are thought to be caused by the plasma pressure gradient due primarily to the enhanced electron temperature, but detailed modelling of these data remains to be performed.

### **2.4.1 Artificial optical emissions**

Artificial optical emissions from the F region (and E region) can be induced by high power radio waves. The easiest emission to be observed is the red line at 630 nm from O(<sup>1</sup>D) which has an excitation threshold energy of 1.97 eV, followed by the green line at 577.7 nm from O(<sup>1</sup>S) with an effective energy threshold of 4.19 eV but lines have also been observed at 844.6 nm, from O(3p<sup>3</sup>P) with threshold of 10.99 eV and at 427.8 nm with threshold 18 eV from N<sub>2</sub><sup>+</sup> [25]. There seem to be two mechanisms involved. The first is the reasonably well understood thermal heating of the electrons causing the Maxwellian tail to be enhanced [12]. With electron heating of 2000-4000K this mechanism can explain the 630 nm red-line emission of atomic oxygen which has the lowest excitation energy. The other mechanism, which is not well understood, is the acceleration of thermal electrons to supra-thermal energies of up to a few tens of eV by a process involving plasma waves. This second mechanism seems necessary to explain the green line (577.7 nm) atomic oxygen emission and other emissions at 844.6 nm and 427.8 nm with higher energy thresholds.

Whatever the mechanism, it is possible to create a cloud of excited atomic oxygen atoms which can be used to determine thermospheric properties as described by [26]. For example, steady state heating causes the cloud of optical emission to move with the plasma velocity ( $\mathbf{E} \times \mathbf{B}$  drift) and show the irregularity structure of the plasma. When the radio wave is turned off, the cloud expands by neutral diffusion drifts and drifts with the neutral wind velocity as the intensity decays on a timescale of tens of seconds. The decay rate is determined by the collisional quenching rate and both diffusion quenching rates are directly related to the atomic and molecular concentrations in the thermosphere. The accompanying paper by Slanger [27] in this volume gives a more detailed description of the importance of atomic oxygen in both natural and artificially-excited atmospheric airglow measurements. Whereas the neutral wind probably does not vary much with height, the neutral density decreases with height causing the lifetime of the excited O state and the diffusion rate to decrease with height. Thus by measuring the decay of artificial red line emissions at different heights one could obtain a height profile of the neutral density. Some initial measurements which could be used in an attempt to do this is shown in Figure 5, taken from [28], where the optical emission height increased as the ionosphere decayed after sunset. In such experiments it is necessary to determine the height of the optical emissions by triangulation using several cameras. Alternatively one could estimate the height from the HF reflection altitude, but the two heights are not necessarily the same. The source height of the electron heating or electron acceleration, which is the upper-hybrid resonance height which is close to but below the HF reflection height, can usually be determined from ionosonde or radar measurements.

## **3.0 PLASMA WAVE EXCITATION**

The electric field of the powerful HF wave becomes even stronger near the reflection height as a result of

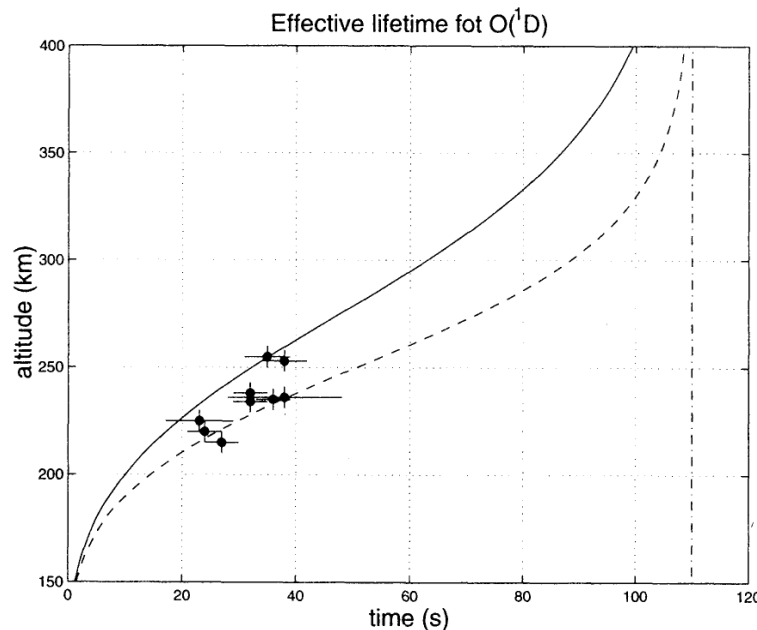


**Figure 5: Altitude variation of the decay time constants of O(<sup>1</sup>D) from [26]. The dot-dashed line shows the radiative lifetime of O(<sup>1</sup>D), the dashed curve including quenching by O<sub>2</sub>, N<sub>2</sub> and ambient electrons, the solid curve including quenching by atomic oxygen. The markers show estimates of the time constant from the experiment described in [28].**

the decreasing refractive index. It can decay into ion acoustic and Langmuir waves both of which may be detected by incoherent scatter radars and thereby provide a strong signal, in a usually very narrow range interval which is ideal for calibrating electron density measurement of such radars. Often it is even possible to obtain such enhanced ion and plasma lines on the topside ionosphere, through tunnelling of the HF wave in the Z-mode [29].

The daughter waves of the HF electromagnetic wave decay, namely the ion acoustic and Langmuir waves, can themselves be strong enough to decay into other ion acoustic and Langmuir waves of oppositely directed wave-number, leading to a cascading process. This whole process is very similar to the natural amplification or generation of Langmuir waves by precipitating or backscattered soft electrons of a few eV. It is thought that electron beams associated with the aurora can also excite Langmuir and ion-acoustic waves [30]. Therefore the same radar techniques and simulations of the plasma processes can be used for studying both HF-induced plasma waves and naturally occurring Langmuir turbulence. An example of both aurorally-enhanced and HF-enhanced Langmuir and ion acoustic waves is shown in Figure 1 of Rietveld et al. [31]. Many papers have been written on the subject of these plasma instabilities, often termed Langmuir turbulence, but here we will not go into that subject further.

## 4.0 ULF, ELF, VLF WAVE EXCITATION AND DETECTION

### 4.1 Excitation of ELF/VLF waves

The production of ELF/VLF waves (from hundreds of Hz to many kHz) by modulated heating and thereby conductivity modulation in the lower layers of the ionosphere provides a number of diagnostic techniques. An advantage of this source of low frequency waves is its wide instantaneous bandwidth in spite of the

low efficiency [32]. One approach is to use the radiated ELF/VLF waves propagating in the Earth-ionosphere waveguide to test models of propagation and models of the lower ionosphere, as done by Barr et al. for example [33]. Since the height region of the modulated currents in the ELF/VLF range is between 55 and 90 km, depending on conditions [34][35] local observations of the ELF/VLF waves give information on the wave production processes and thereby on the ionosphere at these heights.

The nonlinear relationship between electron temperature enhancement and HF energy input depends on the loss mechanism of the heated electrons. For small electron temperature enhancements, rotational excitation of  $N_2$  and  $O_2$  is the most efficient energy loss mechanism. Its temperature dependence is known to be  $(T_e - T_n)/T_e^{1/2}$  where  $T_e$  and  $T_n$  are the electron and neutral temperatures respectively. Since the collision frequency  $\nu_e$  is approximately proportional to  $T_e$ , there exists an altitude above which the HF absorption coefficient increases with  $T_e$  more strongly than  $T_e^{1/2}$ . It is obvious that in this case there is a critical energy input above which the loss cannot compensate the gain. Correspondingly, a runaway solution for  $T_e$  arises, which is eventually limited by other energy loss mechanisms, mainly vibrational excitation of  $N_2$  and  $O_2$ . This relationship could be measured by seeing how the amplitude of waves at a fixed ELF/VLF modulation frequency having a fixed modulation depth varies as the average HF level is increased, as outlined in [34]. Although there have been many ELF/VLF modulation experiments performed over the years, this particular one has not been done, but it could provide the shape of the  $T_e$  vs. HF-power curve which one should be able to relate to the model containing the height profile of  $[O_2]$ ,  $[N_2]$  and  $T_n$ .

### 4.2 Excitation of ULF waves

The production of ULF waves below about 10 Hz is particularly interesting because there are so few alternative artificial sources. These waves, as they propagate into the magnetosphere as Alfvén waves, can be very efficiently guided along the magnetic field to satellites and thereby provide a tracer of the field line [36], [37]. Such spatially localised ULF waves originating from the electrojet can acquire a significant parallel electric field as they propagate up into the magnetosphere, and can thereby accelerate electrons in a process which may be analogous to natural auroral processes [36]. These ULF waves fall into the frequency range of, and may therefore be used to actively study, the ionospheric Alfvén resonator [38], [39], [40] which is a region along the magnetic field bounded by the ionosphere at the bottom and at the top by a peak in the Alfvén speed at an altitude of about 0.5 Earth radii.

### 4.3 Detection of natural ULF waves using heating

There are at least two ways of detecting the ionospheric signature of naturally occurring ULF pulsations. The first way is by the fact that the electric field of the natural ULF wave modulates the current system in the lower ionosphere thereby imparting its frequency on any ELF or VLF waves that may be produced by artificial modulation of those currents. Signatures of natural Pc 4 and Pc 1 ULF waves were thus found on the amplitude and phase of ELF/VLF waves produced by the HF facility and recorded on the ground nearby [41], [42]. These ULF waves were also seen by ground-based magnetometers so that they were not shielded by the ionosphere.

Another, more interesting technique can be used to detect the ionospheric signature in the F region of pulsations that have such a localised spatial scale that they are not normally observable by ground based magnetometers because of the shielding effect of the ionosphere. It involves generating decameter scale irregularities near the upper-hybrid resonance height using o-mode heating, and then detecting the movement of the irregularities with coherent radars like SUPER DARN as shown in [43]. The horizontal electric fields of the pulsation cause an  $\mathbf{E} \times \mathbf{B}$  force on the plasma containing the artificial irregularities resulting in a Doppler shift of coherently scattered radar signals. The artificial irregularities have a very narrow intrinsic backscatter spectrum [44], allowing high precision measurements of the drifts. In order to use this technique one does not need a very powerful HF facility. At EISCAT this experiment is commonly performed using only about half of the transmitters and antennas so as to get a wider heater beam and hence a wider region of irregularity generation. This also reduces the power consumption during

the continuous transmission over several hours.

### 5.0 PROBING OF ARTIFICIAL PERIODIC IRREGULARITIES

A particularly powerful method of using heating facilities to probe the ionosphere from the reflection height of the HF wave down to 50 km or so is the artificial periodic irregularity (API) technique developed by a Russian group using the SURA HF facility [45]. The technique relies on the standing wave pattern created by the HF wave and its reflection causing a horizontally stratified periodic perturbation to the refractive index which is then probed by pulsed HF radio waves matching the Bragg scattering criterion, as illustrated in Figure 6. This probing can be performed with the same frequency and polarisation as the pump wave so that the Bragg condition is met at all heights. In this case the probing can only be done to watch the irregularity pattern decay immediately after the pump switches off. Alternatively, the probing can be done with another frequency and polarization such that the Bragg condition is met over a narrow range of heights, but while the pump wave is on. The first mode is

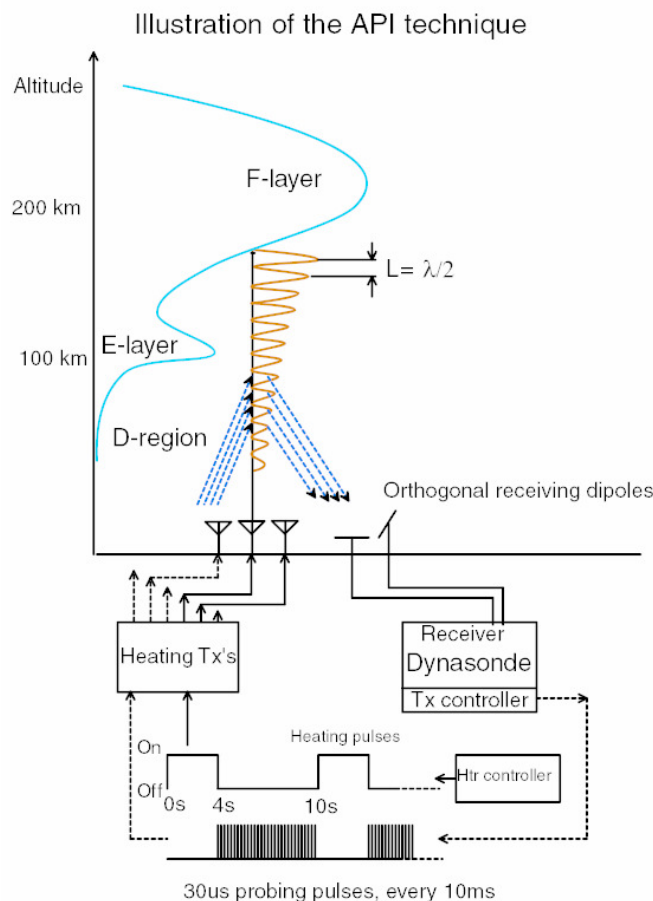
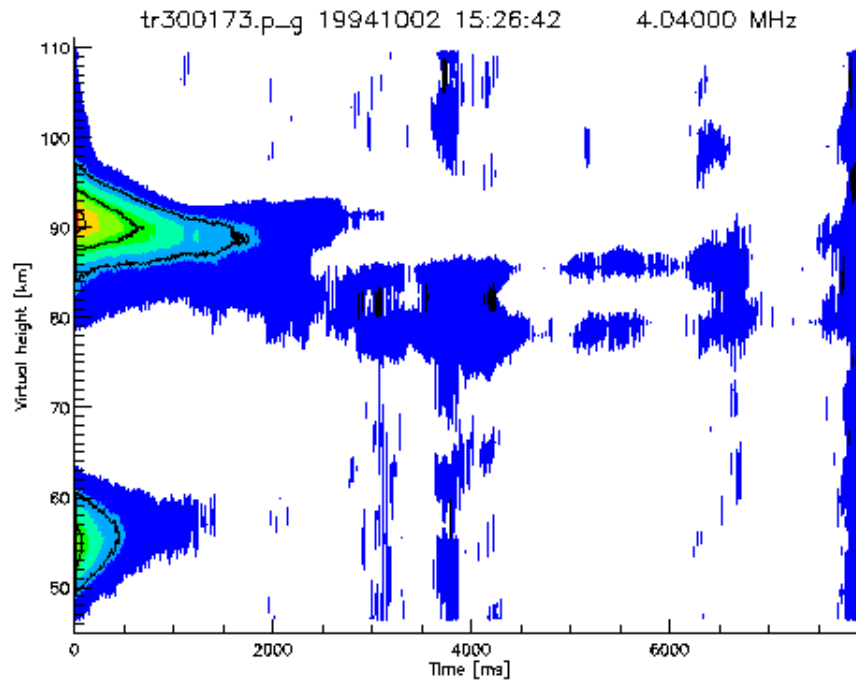


**Figure 6: Illustration of the single-frequency API experiment setup at Tromsø. The heating transmitters are used both for creating the pump standing wave and for transmitting the probing wave. In principle Bragg scattering is possible up to the reflection height as long as the irregularities are formed and have a long enough decay time.**



19941002 15:26:42 pulses 4800 to 5595

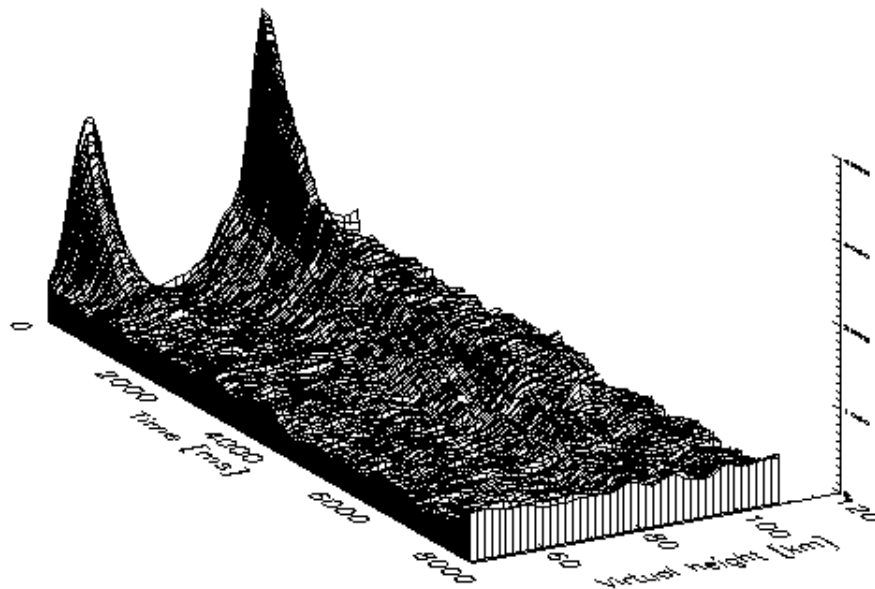


Figure 7: Very low altitude echoes between 50 and 60 km as well as more common echoes between 80 and 110 km from decaying irregularities after turning off the standing wave pattern caused by the powerful HF wave and its ionospheric reflection.

appropriate for D region heights where the time constant for irregularities to decay is generally long enough. An example is shown in Figure 7 where irregularities are formed in two height regions, 80-100 km and 50-60 km and decay with different time constants which are determined by the ion chemistry [46]. In addition to measuring the amplitude decay, the rate of change of phase can also be measured giving the Doppler shift or vertical velocity of the atmosphere in which the decaying irregularities are embedded [46].

## 6.0 SUMMARY

I have tried to show that HF-heating facilities can be used for much more than just plasma physics experiments; namely that HF-heating can be used to learn about the atmosphere, ionosphere and even magnetosphere. Many of the techniques outlined here have been tried to some extent, but there is still a large potential to exploit them in a more systematic way. I hope this will happen both at EISCAT and at the other HF facilities around the world.

## 7.0 ACKNOWLEDGEMENTS

I thank the very many colleagues who helped obtain the results presented here. The EISCAT Scientific Association is supported by the Suomen Akatemia of Finland, the Centre National de la Recherche Scientifique of France, the Max-Planck Gesellschaft of Germany, the National Institute of Polar Research of Japan, the Forskningsråd of Norway, the Naturvetenskapliga Forskningsråd of Sweden, and the Particle Physics and Astronomy Research Council of the United Kingdom.

## 8.0 REFERENCES

- [1] Tellegen, B.D.H. (1933). *Interaction between radio waves?* Nature, 131, 840.
- [2] Bailey, V.A. & Martyn, D.F. (1934). *Influence of electric waves in the ionosphere.* Phil. Mag., 23, 369.
- [3] Fejer, J. (1955). *The interaction of pulsed radio waves in the ionosphere.* J. Atmos. Terr. Phys., 7, 322-332.
- [4] Fejer, J. (1970). *Radio wave probing of the lower ionosphere by cross-modulation techniques.* J. Atmos. Terr. Phys., 32, 597-607.
- [5] Wong, A.Y., Carroll, J., Dickman, R. et. al. (1990). *High-power radiating facility at the HIPAS observatory.* Radio Science, 25, 1269-1282.
- [6] Pedersen, T.R. & Carlson, H.C. (2001). *First observations of HF heater-produced airglow at the High Frequency Active Auroral Research Program facility: Thermal excitation and spatial structuring.* Radio Sci., 36, 5, 1013-1026.
- [7] Rietveld, M.T., Kohl, H. Kopka, H. & Stubbe, P. (1993). *Introduction to ionospheric heating experiments at Tromsø Part 1: Experimental overview.* J. Atmos. Terr. Phys., 55, 577-599.
- [8] Robinson, T.R., Yeoman, T.K., Dhillon, R.S., Lester, M., Thomas, E.C., Thornhill, J.D., Wright, D.M., van Eyken, A.P. & McCrea, I. (2006). *First observations of SPEAR induced artificial backscatter from CUTLASS and the EISCAT Svalbard radar.* Annales Geophysicae, 24, 291-309.
- [9] Frolov V.L., Sergeev, E.N., Komrakov, G.P., Stubbe, P., Thidé, B., Waldenvik, M., Veszelei, E. &

- Leyser, T.B. (2004). *Ponderomotive narrow continuum (NC p) component in stimulated electromagnetic emission spectra*. J. Geophys. Res., 109, A07304, doi:10.1029/2001JA005063.
- [10] Fejer, J. A., Sulzer, M.P. & Djuth, F.T. (1991). *Height dependence of the observed spectrum of radar backscatter from HF-Induced ionospheric langmuir turbulence*. J. Geophys. Res., 96(A9), 15985-16008.
- [11] Robinson, T.R., Bond, G., Eglitis, P., Honary, F. & Rietveld, M.T. (1998). *RF heating of a strong auroral electrojet*. Adv. Space Res., 21, 5, 689-692.
- [12] Mantas, G.P., Carlson Jr., H.C. & LaHoz, C.H. (1981). *Thermal response of the F region ionosphere in artificial modification experiments by HF radio waves*. J. Geophys. Res., 86, 561-574.
- [13] Rietveld, M.T., Kosch, M.J., Blagoveshchenskaya, N.F., Kornienko, V.A., Leyser, T.B. & Yeoman, T.K. (2003). *Ionospheric electron heating, optical emissions and striations induced by powerful HF radio waves at high latitudes: aspect angle dependence*. J. Geophys. Res., 108, A4, (SIA 2-1 to SIA 2-16), 1141, doi:10.1029/2002JA009543.
- [14] Sulzer, M., Tomko, A., Ferraro, A.J. & Lee, H.S. (1976). *Complementary cross-modulation: A new technique for ionospheric modification studies*. J. Geophys. Res., 81, 25, 4754-4756.
- [15] Röttger, J., LaHoz, C., Kelley, M.C., Hoppe, U.-P. & Hall, C., (1988). *The structure and dynamics of polar mesosphere summer echoes observed with the EISCAT 224-MHz radar*. Geophys. Res. Lett., 15, 1353-1356.
- [16] Cho, J.Y.N. & Kelley, M.C. (1993). *Polar mesosphere summer radar echoes: Observations and current theories*. Rev. Geophys., 31, 3, 243-265.
- [17] Kirkwood, S., Barabash, V., Belova, E., Nilsson, H., Rao, T.N., Stebel, K., Osepian, A. & Chilson, P.B. (2002). *Polar mesosphere winter echoes during solar proton events*. Advances in Polar Upper Atmosphere Research, 16, 111-125.
- [18] Chilson, P.B., Belova, E., Rietveld, M.T., Kirkwood, S. & Hoppe, U.-P. (2000). *First artificially induced modulation of PMSE using the EISCAT heating facility*. Geophys. Res. Lett., 27, 23, 3801-3804.
- [19] Belova, E., Chilson, P.B., Kirkwood, S. & Rietveld, M.T. (2003). *The response time of PMSE to ionospheric heating*. J. Geophys. Res. 108, D8, (PMR 13-1 to PMR 13-6), 8446, doi:10.1029/2002JD002385.
- [20] Rietveld, M.T., Kopka, H., & Stubbe, P. (1986). *D-region characteristics deduced from pulsed ionospheric heating under auroral electrojet conditions*. J. Atmos. Terr. Phys., 48, 4, 311-326.
- [21] Rapp, M. & Lübken, F.-J. (2000). *Electron temperature control of PMSE*. Geophys. Res. Lett., 27, 20, 3285-3288.
- [22] Havnes, O. (2004). *Polar Mesospheric Summer Echoes (PMSE) overshoot effect due to cycling of artificial electron heating*. J. Geophys. Res., 109, A02309, doi:10.1029/2003JA010159.
- [23] Havnes, O., La Hoz, C., Naesheim, L.I. & Rietveld, M.T. (2003). *First observations of the PMSE overshoot effect and its use for investigating the conditions in the summer mesosphere*. Geophys. Res.

Lett. 30, 23, 2229, doi:10.1029/2003GL018429.

- [24] Stocker, A.J., Honary, F., Robinson, T.R., Jones, T.B., Stubbe, P. & Kopka, H. (1992). *EISCAT observations of large scale electron temperature and electron density perturbations caused by high power HF radio waves*. J. Atmos. Terr. Phys., 54, 11/12, 1555-1572.
- [25] Gustavsson, B., Sergienko, T., Kosch, M.J., Rietveld, M.T., Brändström, B.U.E., Leyser, T.B., Isham, B., Gallop, P., Aso, T., Ejiri, M., Grydeland, T., Steen, Å., LaHoz, C. Kaila, K., Jussila, J. & Holma, H. (2005). *The electron energy distribution during HF pumping, a picture painted with all colors*. Ann. Geophysicae, 23, 1747-1754.
- [26] Bernhardt, P.A., Wong, M., Huba, J.D., Fejer, B.G., Wagner, L.S., Goldstein, J.A., Selcher, C.A., Frolov, V.L., and Sergeev, E.N. (2000). *Optical remote sensing of the thermosphere with HF pumped artificial airglow*. J. Geophys. Res., 105, 10 657-10 671.
- [27] Slinger, T.G. (2006). *Studies of Ionospheric Processes in the Atmosphere and the Laboratory*. Paper presented at IST056 meeting, 12-16 June 2006, Fairbanks, Alaska. This CD.
- [28] Gustavsson, B., Sergienko, T., Rietveld, M.T., Honary, F., Steen, Å., Brändström, B.U.E. Leyser, T.B., Aruliah, A., Aso, T., Ejiri, M. & Marple, S. (2001). *First tomographic estimate of volume distribution of HF-pump enhanced airglow emission*. J. Geophys. Res., 106, A12, 29105-29124.
- [29] Isham, B., Kofman, W., Hagfors, T., Nordling, J., Thidé, B., LaHoz, C. & Stubbe, P. (1990). *New phenomena observed by EISCAT during RF ionospheric modification experiments*. Radio Sci., 25, 3, 251-262.
- [30] Forme, F., Ogawa, Y., & Buchert, S.C. (2001). *Naturally enhanced ion acoustic fluctuations at different wavelengths*. J. Geophys. Res., 106, A10, 21503-21515.
- [31] Rietveld, M.T., Isham, B., Grydeland, T., La Hoz, C., Leyser, T.B., Honary, F., Ueda, H., Kosch, M., Hagfors, T. (2002). *HF-Pump-Induced Parametric Instabilities in the Auroral E-Region*. Adv. Space Res., 29, 9, 1363-1368.
- [32] Barr, R., Rietveld, M.T., Kopka, H., Stubbe, P. & Nielsen, E. (1985). *Extra-low-frequency radiation from the polar electrojet antenna*. Nature, 317, 6033, 155-157.
- [33] Barr, R., Stubbe, P., Rietveld, M.T. & Kopka, H. (1986). *ELF and VLF Signals Radiated by the 'Polar Electrojet Antenna': Experimental Results*. J. Geophys. Res., 91, A4, 4451-4459.
- [34] Stubbe, P., Kopka, H., Rietveld, M.T. & Dowden, R.L. (1982). *ELF and VLF wave generation by modulated heating of the current carrying lower ionosphere*. J. Atmos. Terr. Phys., 44, 12, 1123-1135.
- [35] Rietveld, M.T., Mauelshagen, H.-P., Stubbe, P., Kopka, H., & Nielsen, E. (1987). *The Characteristics of Ionospheric Heating-Produced ELF/VLF Waves Over 32 Hours*, J. Geophys. Res., 92, A8, 8707-8722.
- [36] Robinson, T.R., Strangeway, R., Wright, D.M., Davies, J.A., Horne, R.B., Yeoman, T.K., Stocker, A.J., Lester, M., Rietveld, M.T., Mann, I.R., Carlson, C.W. & McFadden, J.P. (2000). *FAST observations of ULF waves injected into the magnetosphere by means of modulated RF heating of the auroral electrojet*. Geophys. Res. Lett. 27, 3165-3168.

- [37] Wright, D.M., Davies, J.A., Robinson, T.R., Yeoman, T.K., Lester, M., Cash, S.R., Kolesnikova, E., Strangeway, R., Horne, R.B., Rietveld, M.T. & Carlson, C.W. (2003). *The tagging of a narrow flux tube using artificial ULF waves generated by modulated high power radio waves*. J. Geophys. Res. 108, 1090, doi:10.1029/2002JA009483.
- [38] Cash, S.R., Davies, J.A., Kolesnikova, E., Robinson, T.R., Wright, D.M., Yeoman, T.K. & Strangeway, R.J. (2002). *Modelling electron acceleration within the IAR during a 3 Hz modulated EISCAT heater experiment and comparison with FAST satellite electron flux data*. Ann. Geophys., 20, 1499-1507.
- [39] Kolesnikova, E., Robinson, T.R., Davies, J.A., Wright, D.M., Lester, M. (2002). *Excitation of Alfvén waves by modulated HF heating of the ionosphere, with application to FAST observations*. Ann. Geophys., 20, 57-67.
- [40] Bösinger, T., Kero, B., Pollari, P., Pashin, A., Belyaev, P., Rietveld, M., Turunen, T. & Kangas, J. (2000). *Generation of artificial magnetic pulsations in the Pc1 frequency range by periodic heating of the Earth's ionosphere: indications of Alfvén resonator effects*. J. Atmos Solar Terr. Physics., 62, 4, 277-297.
- [41] Rietveld, M.T., Kopka, H., Nielsen, E., Stubbe, P. & Dowden, R.L. (1983). *Ionospheric electric field pulsations: a comparison between VLF results from an ionospheric heating experiment and STARE*. J. Geophys. Res. 88, 2140-2146.
- [42] Rietveld, M.T., Kopka, H. & Stubbe, P. (1988). *Pc1 ionospheric electric field oscillations*. Ann. Geophys. 6, 381-388.
- [43] Wright, D.M. & Yeoman, T.K. (1999). *High-latitude HF Doppler observations of ULF waves. 2. Waves with small spatial scale sizes*. Ann. Geophys. 17, 868-876.
- [44] Eglitis, P., Robinson, T.R., Rietveld, M.T., Wright, D.M. & Bond, G.E. (1998). *The phase speed of artificial field-aligned irregularities observed by CUTLASS during HF modification of the auroral ionosphere*. J. Geophys. Res., 103 , A2, 2253-2259.
- [45] Belikov, V.V., Benediktov, E.A., Tolmacheva, V. & Bakhmet'eva, N.V. (2002). *Ionospheric research by means of artificial periodic irregularities*. English edition (translated by M. Förster and M.T. Rietveld), Copernicus GmbH (D-37191 Katlenburg-Lindau, Germany), ISBN 3-936586-03-9, 160 pages.
- [46] Rietveld, M.T., Turunen, E., Matveinen, M., Goncharov, N.P. & Pollari, P. (1996). *Artificial Periodic Irregularities in the Auroral Ionosphere*. Ann. Geophysicae 14, 1437-1453.